Asian Journal of Chemistry; Vol. 38, No. 8 (2026), 2037-2044
ASIAN JOURNAL OF CHEMISTRY
https://doi.org/10.14233/ajchem.2026.36220

Galvanostatic Deposition of Polyaniline on Mild Steel in Benzoic Acid – Alcohol Water System and Its Corrosion Performance in Na_2SO_3 Medium

DIPAK KUMAR GUPTA[1], ANJU KUMARI DAS[2,*], GAYATRI MAIYA KOJU[3], SANJAY SINGH[1,2,*] and AMAR PRASAD YADAV[1]

[1]Central Department of Chemistry, Tribhuvan University, Kirtipur, Kathmandu, Nepal
[2]Department of Chemistry, Tribhuvan University, Amrit Science Campus, Kathmandu, Nepal
[3]Department of Chemistry, Tribhuvan University, Bhaktapur Multiple Campus, Bhaktapur, Nepal

*Corresponding authors: E-mail: anjudas004@gmail.com; thesanjaysingh@gmail.com

Received: 14 April 2026 *Accepted*: 17 June 2026 *Published online*: 7 August 2026 AJC-22429

The polyaniline (PANI) coating on a mild steel (MS) surface, prepared from 0.3 M aniline in 0.04 M benzoic acid in a 3:1 alcohol-water (BAW) solvent, was investigated by the galvanostatic method. The influence of current density on the development of a homogeneous and adherent PANI coating on MS was explored at current densities of 100, 200 and 300 μA cm^{-2}. The results showed a sequential process of MS dissolution, benzoate salt formation, oxidation of the aniline monomer and PANI coating nucleation and growth. The corrosion behaviour of the PANI coating was examined using potentiodynamic polarisation (PDP) and electrochemical impedance spectroscopy (EIS) in a 0.4 M Na_2SO_3 solution to simulate an industrial environment. The inhibition efficiency of the PANI coating was affected by the applied current density. The best inhibition efficiency of the PANI coating by PDP, obtained at 100 μA cm^{-2}, was approximately 96%, followed by 85% at 200 μA cm^{-2} and 75% at 300 μA cm^{-2}. The EIS showed 99.75% inhibition efficiency, resulting in excellent barrier protection. The PANI film showed stability in 0.4 M Na_2SO_3 solution at a higher anodic potential. The optical and scanning electron microscopic techniques were utilised to investigate the microstructural features and surface morphology of the coatings before and after polarisation exposure.

Keywords: Electropolymerisation, Mild steel, Benzoic acid in alcohol-water, Polyaniline.

INTRODUCTION

Corrosion protection remains a major concern in modern industry because the degradation of metallic materials leads to significant economic losses, resource depletion and safety hazards [1]. Mild steel (MS) is widely used in wires, fencing, automobiles, pipelines, machinery components and construction materials due to its low cost and favourable mechanical properties [2]. Its susceptibility to corrosion has stimulated extensive research on protective coatings. Polymer coatings have attracted considerable attention for MS protection owing to their chemical, optical, environmental, electrical and thermal properties [3-8], together with their ease of preparation and application [9,10]. Among conducting polymers, polyaniline (PANI) has emerged as a promising green anticorrosion material. Electrochemically deposited PANI coatings on active metals have shown excellent corrosion protection due to their environmental compatibility, simple synthesis and favourable protective characteristics [11-15].

Hence, using PANI-based coatings has increased and is considered the best option for metal corrosion protection. PANI protects the MS by preventing etchant penetration and forming a passive primer film on the metal surface. Wessling suggested [16] that PANI and polypyrrole (PPy) conducting polymer coatings may tend to self-heal the passive film between the metal and the coating, which might be naturally restored at defective areas with the oxidation of conductive polymer. The inherent porosity and ion-exchange characteristics of conducting polymer coatings may facilitate electrolyte penetration into the coating matrix, thereby limiting their long-term protective performance [16,17].

Adhesion of the coating to the mild steel substrate plays a crucial role in corrosion protection [18] and this characteristic is strongly influenced by the electrolyte composition and

dopant ions employed during the electropolymerisation of aniline onto the MS surface. Researchers have proposed the use of oxalic acid [19-21], sodium oxalate [22,23], sodium benzoate [24] and sodium salicylate [25] as the electrolytes in the polymerisation of aniline. It has been reported that polyaniline can be deposited after the first oxidation of the MS, which forms an oxalate/salicylate/benzoate pseudopassive layer. This pseudopassive layer can diminish metal dissolution without interfering with the electron transfer process for polymer synthesis [26]. PANI electrosynthesis has primarily been explored with oxalic acid as an electrolyte. However, the oxalate layer does not adequately control iron dissolution; consequently, iron loss and electrolytic bath contamination have been issues.

Our previous study has found sodium potassium tartrate (Na-K tartrate) and benzoic acid in alcohol-water (BAW) as a superior substitute to oxalic acid for PANI coating on MS by the potentiodynamic method [27,28]. The Na-K tartrate medium eliminated the induction period related to mild steel dissolution and lowered the energy requirement for PANI polymerisation and deposition, thereby reducing substrate degradation during coating formation [29].

The present work aims to examine the influence of current density on the deposition behaviour and adhesion characteristics of PANI coatings on MS. Particular attention is given to obtaining compact and adherent PANI films in benzoic acid-water (BAW) electrolyte to improve the corrosion resistance of MS. The protective performance of the coatings was assessed in a simulated industrial environment using 0.4 M Na_2SO_3 as the corrosive medium. Electrochemical measurements showed that aniline oxidation in BAW required only 0.1 mC cm^{-2} of charge for polymerisation initiation. The BAW medium substantially reduced iron dissolution during electropolymerisation and lowered the energy requirement for PANI formation and subsequent coating deposition on the MS surface.

EXPERIMENTAL

Aniline, ethanol and sodium sulphite were purchased from Fisher Scientific, India while benzoic acid was obtained from Merck, India. Aniline was stored in an air-tight, coloured bottle after being freshly distilled before usage. The experiment was conducted at room temperature using solutions prepared in milli water with the requisite concentrations. Commercial-grade mild steel (MS) was cut into 3 cm × 3 cm × 0.15 cm pieces obtained from the local market of Kathmandu, Nepal. After that, the samples were abraded with various grades of silicon carbide (SiC) paper (#100 to #2000) until the MS surface was slick. Before each measurement, the polished MS samples were washed with hexane. The samples were taken in ethanol for ultrasonication for 10 min and dried using compressed air.

Galvanostatic deposition of polyaniline: A potentiostat of Hokuto Denko HA-151 was used for the electrodeposition of PANI on the abraded MS samples [30]. In a three-electrode setup, the MS sample was employed as a working electrode, a saturated calomel electrode (SCE) and graphite electrodes were employed as reference and counter electrodes. Applying an anodic current through an MS sample introduced in 0.3 M aniline containing 0.04 M benzoic acid in 3:1 alcohol-water (BAW) deposited PANI on MS galvanostatically. The current density of 100 μA cm^{-2} to 300 μA cm^{-2} was applied for the deposition of PANI on MS. After polymerisation, the PANI-coated MS was washed with milli water, dried using compressed air and kept in a desiccator for the study.

Surface morphology: Radical Scientific, India, a light polarizing microscope, was applied to study the PANI-coated MS surface morphology in reflection mode with a connected USB ProCam. Before and after polarisation experiments, images of the PANI coatings were taken. The surface morphology of PANI was also established by scanning electron microscope (SEM). The elemental composition of PANI was examined by energy dispersive X-ray spectroscopy (EDX) using a JEM-1200EX electron microscope (JEOL, Japan).

Corrosion test: PANI coating performance for corrosion control was examined in 0.4 M Na_2SO_3 solution by the potentiodynamic technique and electrochemical impedance spectroscopy (EIS). The PANI-coated MS samples were immersed in the test solution for 30 min to obtain a constant open circuit potential (OCP). The potentiodynamic polarisation was carried out by sweeping the potential ± 200 mV from the open circuit potential (OCP) at a scan rate of 1 mV/s. The corrosion inhibition efficiency (IE) was calculated using the eqn. 1:

$$\text{Inhibition efficiency (IE, \%)} = \frac{I_{corr} - I'_{corr}}{I_{corr}} \times 100 \quad (1)$$

where I_{corr} and I'_{corr} are the corrosion current densities of uncoated MS and PANI-coated MS, respectively. The Tafel plot was used to determine the corrosion current and potential.

The EIS was also measured in the CH 660 electrochemical workstation at the OCP. The EIS was recorded using an AC signal of MS and PANI-coated MS in 0.4 M Na_2SO_3 with an amplitude of 10 mV between 100 kHz and 0.01 Hz. Using the ZView 2 software, the experimental findings were analysed. From the Nyquist plot, the charge transfer resistance (R_{ct}) was determined. The fitting analysis substituted the constant phase element (CPE) for the double-layer capacitance (Cdl) to obtain a better fit. The percentage corrosion inhibition efficiency (η%) was determined from eqn. 2:

$$\text{IE (\%)} = \frac{R_{ct} - R^{o}_{ct}}{R_{ct}} \times 100 \quad (2)$$

where the charge transfer resistances of PANI-coated MS and MS are denoted by R^{o}_{ct} and R_{ct}, respectively.

RESULTS AND DISCUSSION

Galvanostatic polymerisation of aniline: The electrochemical deposition of PANI coating on MS was achieved by oxidation of aniline under galvanostatic conditions. The galvanostatic behaviour of MS immersed in 0.3 M aniline + 0.04 M BAW polymerizing solution at current densities of 100 μA cm^{-2}, 200 μA cm^{-2} and 300 μA cm^{-2}, respectively, is shown in Fig. 1. The formation of PANI coating on MS involves three distinct stages, as shown in the potential-time curve: (I) dissolution of MS, (II) formation and growth of the passive film and (III) oxidation and deposition of PANI coating. Fig. 1 shows no induction period is related to MS dissolution and passivation. This property reflects that, unlike oxalic acid,

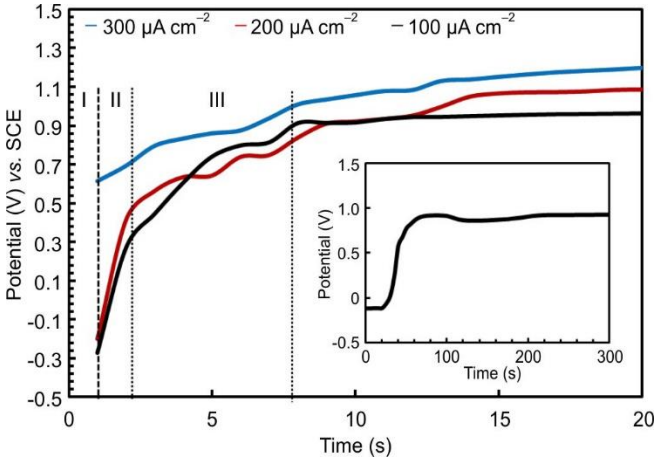

Fig. 1. Galvanostatic coating of a PANI on MS in 0.3 M aniline with 0.04 M BAW at different current densities

which has a distinct induction phase, MS dissolution occurs almost immediately once current is applied (inset in Fig. 1).

The potential remains around -0.270 V during the early phases of polarisation, as shown in Fig. 1 and during stage I, there is a sharp increase in potential, which can be attributed to MS dissolution and the formation of Fe- benzoate. The MS dissolves anodically over time, dependent on the applied current density. The following relationship defines the charge (Q) that passes through the electrode before the potential increases [31,32].

$$Q = I \times t \quad (2)$$

where I is the current density ($\mu A/cm^2$) and t is the time (sec).

In oxalic acid solution, a charge of 275 mC cm^{-2} is required for the oxidation of aniline [31], but in BAW, aniline oxidizes with just 0.1 mC cm^{-2} of charge. As a result, BAW prevents iron loss and reduces the energy required for the polymerisation and subsequent coating of PANI on MS. It subsequently gains in potential (Region II) and a marginal change in potential (Region III).

The MS potential rises as the current density amplifies in the polarisation process represented that metal dissolution decreases as the applied current density rises [33]. The potential increased abruptly from -0.270 V to 0.270 V at a lower current density (100 μA cm^{-2}), then amplified to 0.912 V with effects depicting the passivation and dissolution of MS till 8 sec.

The development of an Fe-benzoate passive film preceded aniline oxidation, which caused a gradual rise in potential and promoted the polymerisation and deposition of PANI. The current density and other experimental parameters, *viz*. media and MS, ascertain the charge needed to oxidize MS [29,34]. For current densities of 200 μA cm^{-2} and 300 μA cm^{-2}, the corresponding potential rose from -0.200 V to 0.634 V in 4 sec and 0.612 V to 0.739 V in 3 sec. A rise in current density causes the passivation of the MS surface. A small drop in potential reveals the passivation, which remains constant due to the continuous growth and surface coverage of PANI.

At a nearly steady potential, small polymerisation was observed on the outer surface. Progression of the polarisation process resulted in a gradual rise in potential and the initiation of external PANI deposition. A prolonged stable potential region followed the formation and thickening of the polymer film. These results are similar to those reported for the electrodeposition of aniline onto MS [31,33,35,36]. Thus, a higher PANI formation rate can be obtained with a higher applied current density.

During the electrochemical deposition of PANI, a radical cation reacts with another radical cation to produce a dimer and combines with an aniline cation to generate polyaniline [37-39]. The proposed reaction mechanism can be summarized as follows: the initial potential region corresponds to the dissolution of iron from the mild steel surface.

$$Fe \rightarrow Fe^{2+} + 2e \quad (3)$$

A passive layer is produced at the MS surface when the Fe^{2+} combines with benzoic acid to form an insoluble Fe-benzoate.

$$Fe^{2+} + C_6H_5COO_2^- \rightarrow (C_6H_5COO)_2Fe\downarrow \quad (4)$$

Following inhibition of metal dissolution, charge transfer became predominantly associated with aniline oxidation and the formation of radical cations responsible for polymer growth. The corresponding increase in potential accompanied the progression of polymerisation. The reaction pathway involving dissolution, passivation, oxidation and polymer formation is summarized below:

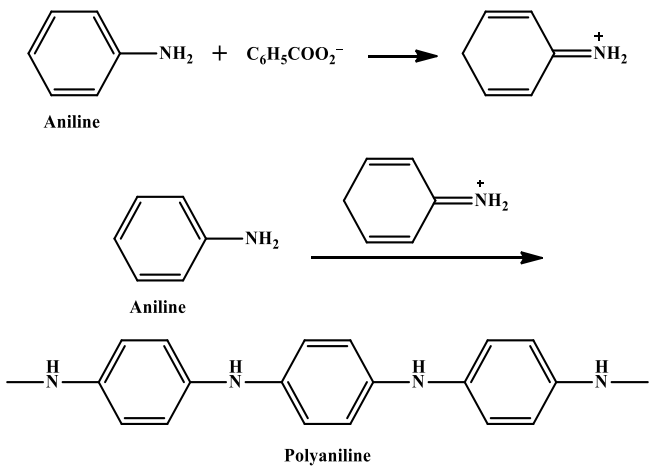

Morphology of PANI coating: The morphology of the electropolymerised PANI coating was strongly influenced by the applied current density. The optical micrographs (Fig. 2a) illustrate the surface appearance of PANI-coated mild steel prepared at different current densities. Deposition at 100 μA cm^{-2} produced a uniform, compact and homogeneous PANI film with good surface coverage. An increase in current density to 300 μA cm^{-2} resulted in a progressive reduction in coating thickness and surface uniformity. The deterioration in coating quality at higher current densities can be attributed to enhanced passivation and oxidation of the mild steel substrate, which reduced the fraction of charge available for aniline oxidation and polymer growth. Partial overoxidation of the deposited PANI may also occur under these conditions, leading to dissolution of brown polymeric species from the outer layer into the electrolyte solution. In contrast, deposition at lower current density favoured controlled polymer growth, resulting in a homogeneous coating composed of uniformly distributed spherical features.

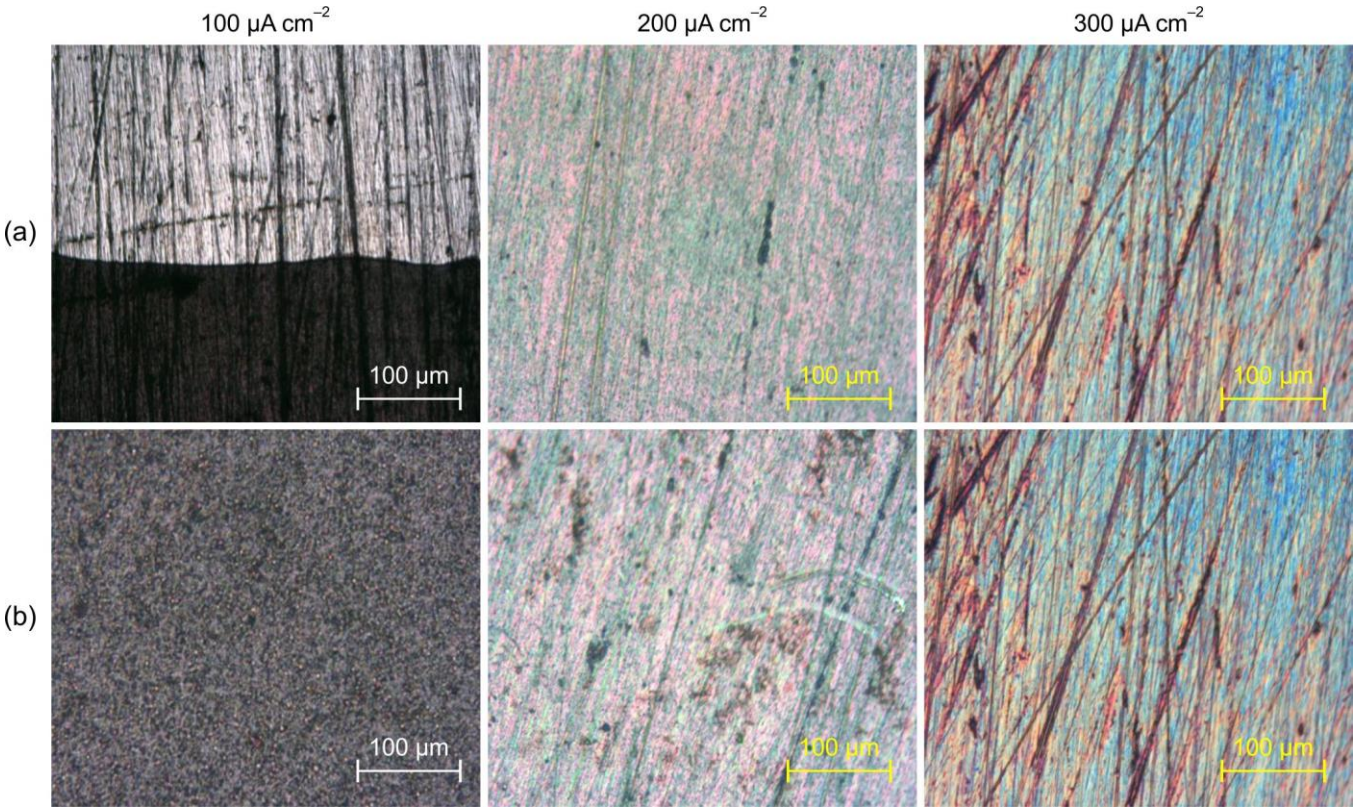

Fig. 2. Optical images of PANI deposited on MS (a) PANI deposited galvanostatically at different current densities (b) after polarizing PANI coating in 0.4 M Na_2SO_3 solution

The surface morphology of the PANI coating deposited at 100 μA cm^{-2} was further examined by SEM and the corresponding micrograph and EDX spectrum are shown in Fig. 3. The SEM image revealed the formation of a thick and compact coating with fine granular features that became distinct only at higher magnifications. The presence of carbon and nitrogen in the EDX spectrum verified the successful deposition of the PANI layer on the mild steel substrate.

Potentiodynamic polarisation in 0.4 M Na_2SO_3: In 0.4 M sodium sulphite, the corrosion behaviour of PANI-coated MS was examined after measuring open circuit potential for 30 min. Potentiodynamic polarisation curves are shown in Fig. 4. The electrochemical parameters measured, such as corrosion current density (I_{corr}), corrosion potential (E_{corr}) and corrosion protection efficiency values, are shown in Table-1.

The uncoated MS shows a substantially higher I_{corr} than the PANI-coated MS. A lower I_{corr} value signifies superior corrosion resistance. For PANI deposited at a current density of 100 μA cm^{-2}, the I_{corr} dropped by nearly 33 times, resulting in a corrosion IE of 96.23%. The corrosion inhibition efficiencies of PANI coatings deposited at 200 and 300 μA cm^{-2} were found to be 85.27% and 75.46%, respectively.

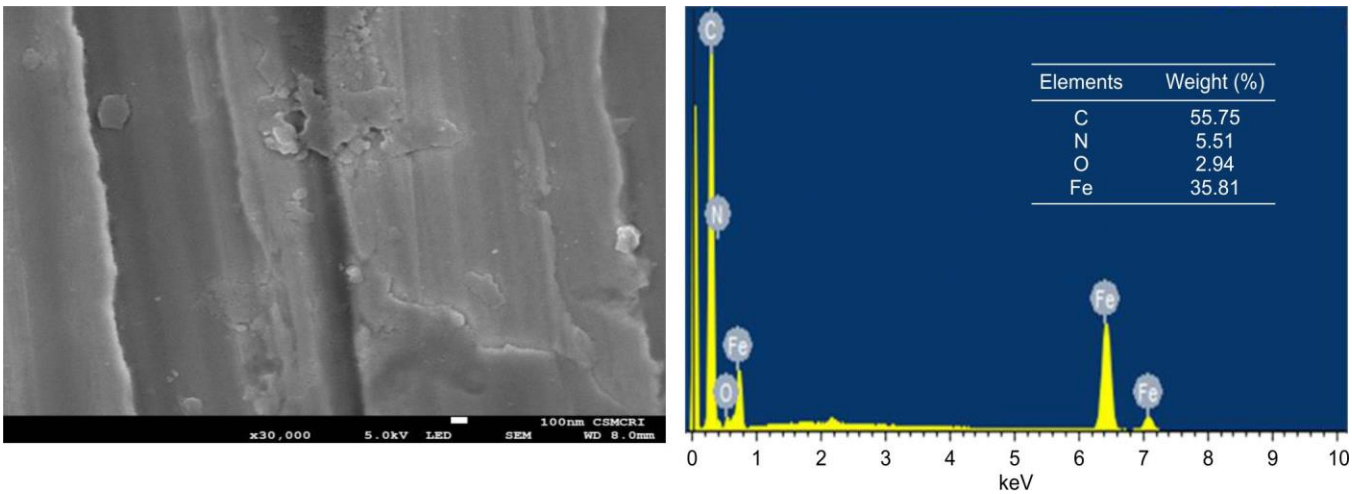

Fig. 3. SEM images of PANI deposited on MS at100 μA cm^{-2} current density and its EDX

TABLE-1
ELECTROCHEMICAL CORROSION PARAMETERS OF PANI-COATED MILD STEEL (MS) AT DIFFERENT CURRENT DENSITIES IN 0.4 M Na_2SO_3 SOLUTION

Current density (μA/cm^2)	β_a (V/decade)	β_c (V/decade)	I_{corr} (mA/cm^2)	E_{corr} (V)	Inhibition efficiency (%)
MS	0.102	-0.116	0.0163	-0.826	–
300	0.082	-0.058	0.004	-0.896	75.46
200	0.074	-0.056	0.0024	-0.876	85.27
100	0.052	-0.056	0.0005	-0.876	96.23

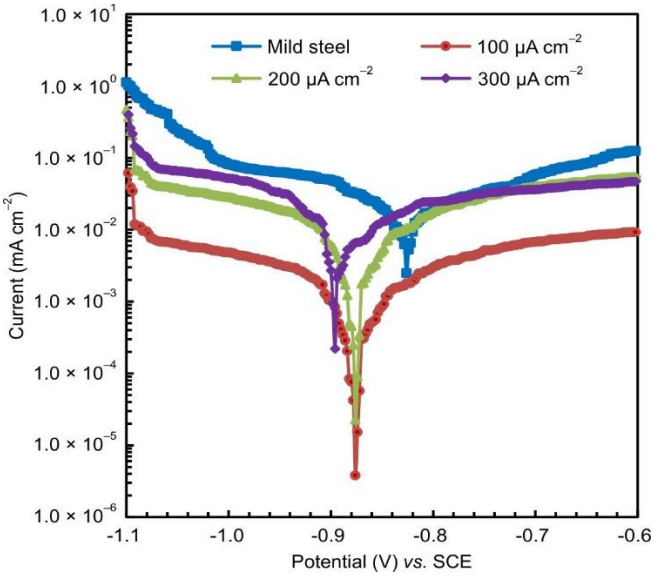

Fig. 4. Corrosion protection behaviour of PANI coating on MS in 0.4 M Na_2SO_3 solution

The anodic and cathodic polarization responses of mild steel do not exhibit ideal Tafel behaviour, with iron dissolution and hydrogen evolution displaying slopes close to 60 mV dec^{-1} and 120 mV dec^{-1}, respectively [40]. The deviation from regular Tafel characteristics arises from the electrochemical activity of PANI, whose redox transitions participate in the corrosion process and modify both anodic and cathodic reactions. The presence of the PANI layer influenced the polarisation behaviour of the substrate in both potential regions. A reduction in anodic Tafel slope was observed with decreasing deposition current density, which can be attributed to the formation of thicker and more compact PANI coatings under these conditions. The increased coating thickness imposed a greater barrier to charge transfer and retarded the anodic dissolution process.

The open-circuit potential (OCP) of PANI-coated mild steel exhibited only minor variations relative to bare MS, although a slight shift towards more negative potentials was observed. The difference in open-circuit potential between the coated and uncoated substrates remained below 85 mV, consistent with the behaviour of a mixed-type inhibitor affecting both anodic metal dissolution and cathodic reduction processes [28].

The optical micrographs presented in Fig. 2b illustrate the changes in coating morphology following polarization in 0.4 M Na_2SO_3 solution. The surface morphology of PANI coatings prepared at 100 and 200 μA cm^{-2} remained largely unchanged after electrochemical testing, with only slight modifications visible in the micrographs. The coating prepared at 300 μA cm^{-2} developed a distinctly altered surface morphology after polarization, which may be associated with enhanced dissolution of the mild steel substrate following local degradation of the PANI layer. The deterioration in protection performance at higher deposition current densities is consistent with the formation of thinner and less uniform coatings observed before polarization. The results indicate that the current density employed during electropolymerisation strongly influences both the morphology and the protective characteristics of PANI coatings deposited on mild steel in the BAW electrolyte system. These observations provide guidance for selecting suitable deposition conditions for obtaining compact and adherent PANI films with improved corrosion resistance. A comparison with PANI coatings synthesized in oxalic acid and other reported coating systems in different corrosive media is presented in Table-2.

TABLE-2
CORROSION PERFORMANCE OF PANI SYNTHESIS IN OXALIC ACID AND OTHER COATING SYSTEMS

PANI coating preparation	Corrosive medium	Findings	Ref.
Galvanostatic PANI in aqueous oxalic acid	0.4 M NaCl + 0.1 M HCl	Very good corrosion protection; better than PPy-coated iron	[21]
Galvanostatic PANI in 0.3 M aniline + 0.2 M sodium potassium tartrate	0.4 M Na_2SO_3	90% Inhibition efficiency	[29]
Galvanostatic PANI in aqueous oxalic acid	0.4 M NaCl + 0.1 M HCl	Strongly adherent films formed through Fe(II)-oxalate passivation layer	[34]
PANI/Epoxy coating	0.1 M H_2SO_4	PANI pretreatment enhanced epoxy performance through passivation	[41]
PANI/Epoxy	3.5 wt.% NaCl, pH 1 and 13	Better than pure epoxy Acidic and alkaline media reduced performance but remained superior to epoxy	[42]
PANI-PPy coating preparation in oxalic acid	0.5 M NaCl	Significant decrease in anodic dissolution current and higher corrosion protection	[43]

The potentiodynamic polarization experiments were extended to an anodic potential limit of -0.3 V to evaluate the stability of the PANI coating under more oxidising conditions. The polarization curve shown in Fig. 5 exhibited a gradual increase in current with increasing potential, without evidence of abrupt current fluctuations or coating failure. The optical image obtained after polarization (Fig. 6) revealed no significant changes in surface morphology and thereby confirmed the stability of the PANI film and its ability to maintain protection at higher positive potentials.

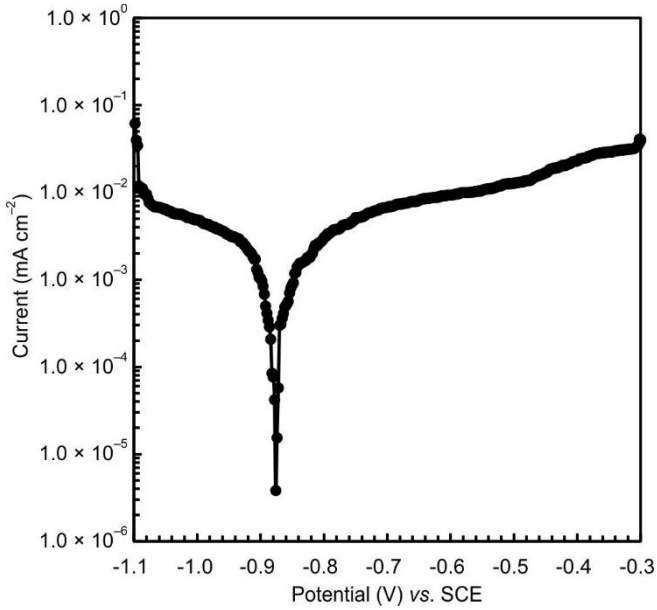

Fig. 5. Potentiodynamic polarisation behaviour of PANI prepared at 100 μA cm^{-2} in 0.4 M Na_2SO_3, revealing the stability of PANI and the passive layer

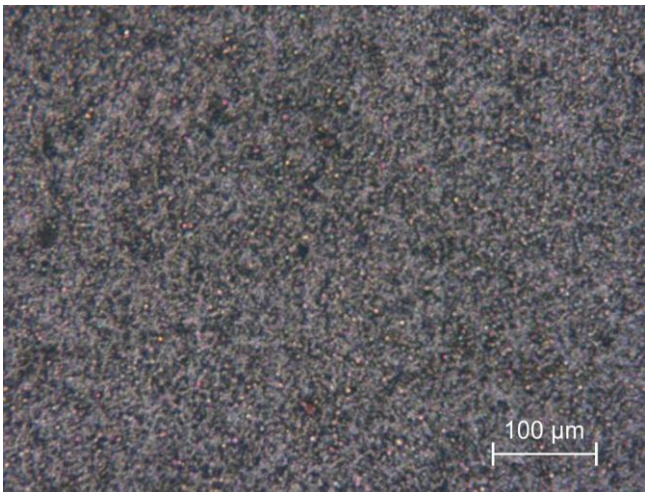

Fig. 6. Optical image of MS coated with PANI potentiodynamically polarised in 0.4 M Na_2SO_3 solution up to -0.3V

EIS studies: Electrochemical impedance spectroscopy (EIS) was used to further examine the corrosion behaviour of PANI-coated MS produced in BAW. The EIS data of PANI coating at 100 μA cm^{-2} in Na_2SO_3 medium is shown in Fig. 7. The experimental EIS data were fitted using an equivalent circuit shown in Fig. 7a. Two parallel RC circuits connected in series with the solution resistance make up the circuit. The factors C_p and R_p define the PANI coating capacitance and coating resistance. Similarly, C_{dl} represents the double-layer capacitance and R_{ct} represents the charge transfer resistance at the metal solution interface.

Table-3 presents the electrochemical impedance data for MS and PANI-coated MS in a 0.4 M Na_2SO_3 solution. PANI-coated MS showed a significant increase in impedance. Deprotonation of PANI in a Na_2SO_3 solution leads to a significant decrease in conductivity. As shown in Fig. 7, the PANI coating substantially increased the impedance response of the mild steel surface. An increased in R_{ct} reflects the suppression of charge transfer reactions and the improved barrier properties of the coating. The corrosion inhibition efficiency in Na_2SO_3 solution reached 99.75%. The increase in phase angle in the Bode-phase plot, the higher impedance modulus at low frequencies and the larger capacitive loop in the Nyquist plot are characteristic of effective corrosion protection by the PANI film. The R_p value increased by more than 8.5 times, while values of n close to unity indicate pseudo-capacitive behaviour at the metal/electrolyte interface [36,37]. EIS investigates both charge transfer and diffusion/mass transfer processes at the electrode surface and adsorption stability or film resistance.

Conclusion

PANI coatings were successfully deposited galvanostatically on mild steel from an electrolyte containing 0.3 M aniline and 0.04 M BAW. The applied current density had a pronounced effect on the thickness, homogeneity and adhesion of the deposited films. Higher current densities exhibited thinner coatings with lower surface uniformity and the presence of pores, which adversely affected their corrosion-protection performance. Deposition at lower current densities favoured the formation of compact, homogeneous and pore-free PANI layers, resulting in a corrosion inhibition efficiency of approximately 96% in 0.4 M Na_2SO_3 solution. The PANI coating prepared in BAW remained stable at potentials more positive than -0.6 V, with no evidence of film breakdown at higher anodic potentials. Electrochemical impedance measurements yielded an inhibition efficiency of 99.75%, accompanied by substantial increases in both polarization resistance (R_p) and charge-transfer resistance (R_{ct}). The electrochemical and morphological results identify BAW as a suitable electrolyte for producing adherent and highly protective PANI coatings on mild steel for corrosion mitigation in sulphite containing environments.

TABLE-3
ELECTROCHEMICAL IMPEDANCE DATA OF MS AND PANI-COATED MS IN 0.4 M Na_2SO_3 SOLUTION

Sample	R_{ct} (Ω)	N	R_p (Ω cm^2)	C_{dl} (μF cm^2)	η (%)
MS	450	0.82	300	25.40	–
PANI	178000	0.90	200000	0.89	99.75

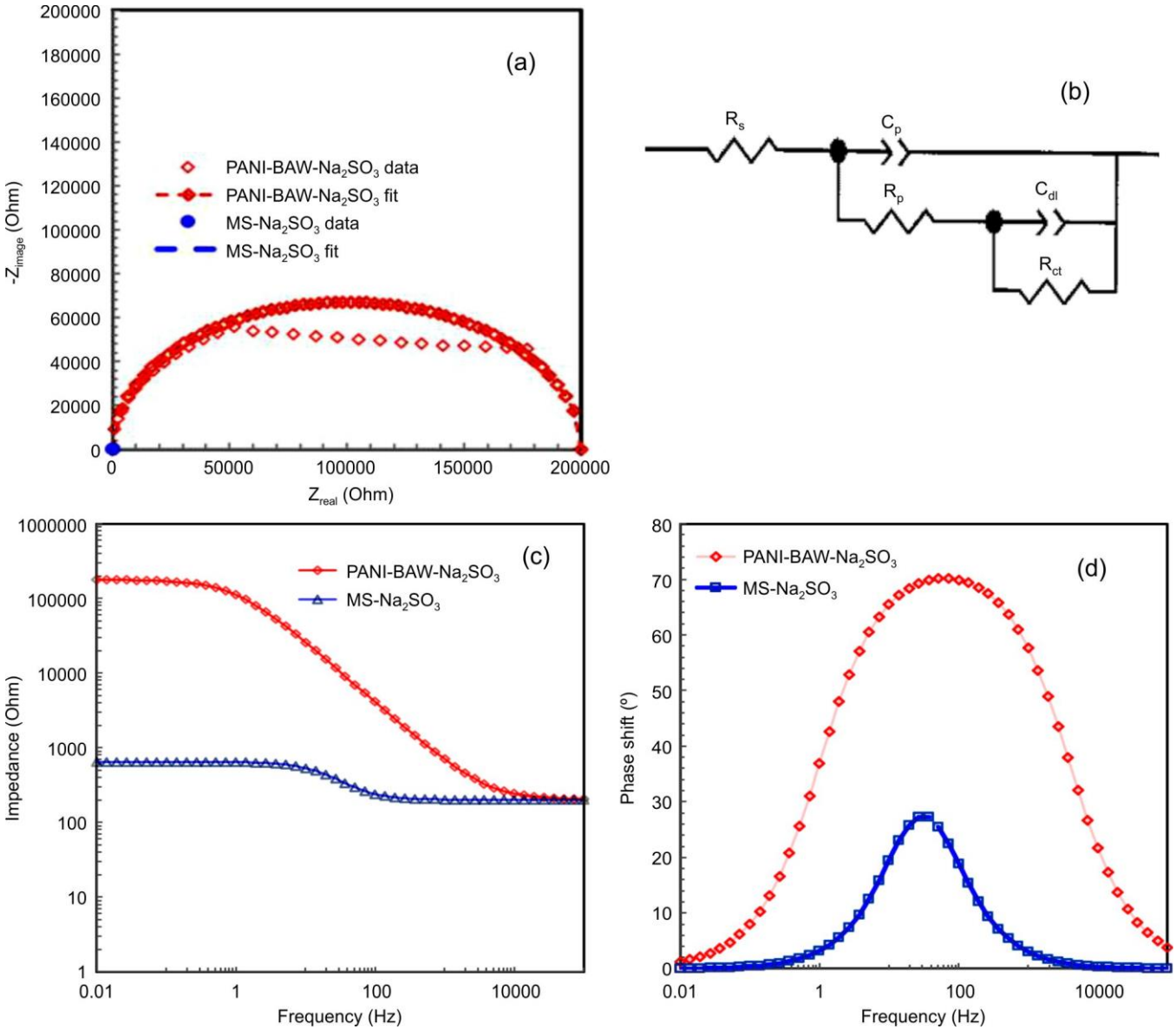

Fig. 7. EIS of MS coated with PANI in BAW immersed in 0.4 M Na_2SO_3 solution (a) Nyquist plot, (b) Equivalent circuit, (c) Bode plot and (d) Phase shift

ACKNOWLEDGEMENTS

One of the authors, D.K. Gupta thank the Nepal Academy of Science and Technology (NAST), Khumaltar, Lalitpur, for supporting this study financially. Central Salt and Marine Chemical Research Institute (CSMCIR)-CSIR, Bhavnagar, India, is also acknowledged for providing SEM-EDX facilities.

CONFLICT OF INTEREST

The authors declare that there is no conflict of interests regarding the publication of this article.

DECLARATION OF AI-ASSISTED TECHNOLOGIES

During the preparation of this manuscript, the authors used an AI-assisted tool(s) to improve the language and no data, results or scientific conclusions were generated by AI. All analyses, interpretations and conclusions are the authors' own. The authors reviewed and edited the content and take full responsibility for the published work.

REFERENCES

1. S. Shi, Y. Zhao, Z. Zhang and L. Yu, *Prog. Org. Coat.*, **132**, 227 (2019); https://doi.org/10.1016/j.porgcoat.2019.03.040
2. A.H. El-Shazly and H.A. Al-Turaif, *Int. J. Electrochem. Sci.*, **7**, 11 (2012).
3. A. Cook, A. Gabriel and N. Laycock, *J. Electrochem. Soc.*, **151**, B529 (2004); https://doi.org/10.1149/1.1782077
4. J. Xu, Y. Zhang, D. Zhang, Y. Tang and H. Cang, *Prog. Org. Coat.*, **88**, 84 (2015); https://doi.org/10.1016/j.porgcoat.2015.06.024
5. A. Akdag, G. Ozyilmaz and A.T. Ozyilmaz, *Anti-Corros. Methods Mater.*, **65**, 580 (2018); https://doi.org/10.1108/ACMM-04-2018-1922
6. N. Huang, C. Liang and B. Yi, *Mater. Corros.*, **59**, 21 (2008); https://doi.org/10.1002/maco.200704062

7. P. Li, T.C. Tan and J.Y. Lee, *Synth. Met.*, **88**, 237 (1997); https://doi.org/10.1016/S0379-6779(97)03860-5
8. M.F.D. Aguiar, R.A. Borges, M.F.B. Rocha, N. Bouchonneau, C.P.D. Melo, H.P.D. Oliveira and K.G.B. Alves, *Mater. Res.*, **26(suppl 1)**, e20220549 (2023); https://doi.org/10.1590/1980-5373-mr-2022-0549
9. E. Kim, N. Kang, J.J. Moon and M. Choi, *Bull. Korean Chem. Soc.*, **37**, 1445 (2016); https://doi.org/10.1002/bkcs.10887
10. Y. Wang, S. Zhang, P. Wang, Z. Lu, S. Chen and L. Wang, *Prog. Org. Coat.*, **137**, 105327 (2019); https://doi.org/10.1016/j.porgcoat.2019.105327
11. M. Ates, *J. Adhes. Sci. Technol.*, **30**, 1510 (2016); https://doi.org/10.1080/01694243.2016.1150662
12. A.M. Abdel-Gaber, B.A. Abd-El-Nabey, E. Khamis, R.M. Salman, H.T. Rahal and Z. El Morr, *Chem. Eng. Commun.*, **1**, (2020); https://doi.org/10.1080/00986445.2019.1710493
13. F. Masdarolomoor, S. Hajizadeh, M. Arab Chamjangali and P.C. Innis, *Synth. Met.*, **250**, 121 (2019); https://doi.org/10.1016/j.synthmet.2019.03.011
14. M.M. Popović and B.N. Grgur, *Synth. Met.*, **143**, 191 (2004); https://doi.org/10.1016/j.synthmet.2003.12.022
15. A.T. Ozyilmaz and A. Akdag, *IMF*, **89**, 215 (2011); https://doi.org/10.1179/174591911X13077162170188
16. B. Wessling, *Adv. Mater.*, **6**, 226 (1994); https://doi.org/10.1002/adma.19940060309
17. M. Sabouri, T. Shahrabi, H.R. Faridi and M.G. Hosseini, *Prog. Org. Coat.*, **64**, 429 (2009); https://doi.org/10.1016/j.porgcoat.2008.08.003
18. A. Truncali, T. Laxminarayan, N. Rajagopalan, C.E. Weinell, S. Kiil and M. Johansson, *J. Coat. Technol. Res.*, **21**, 1875 (2024); https://doi.org/10.1007/s11998-023-00899-9
19. A.M. Fenelon and C.B. Breslin, *Surf. Coat. Technol.*, **190**, 264 (2005); https://doi.org/10.1016/j.surfcoat.2004.04.083
20. N.M. Martyak, P. McAndrew, J.E. McCaskie and J. Dijon, *Prog. Org. Coat.*, **45**, 23 (2002); https://doi.org/10.1016/S0300-9440(02)00070-X
21. J.L. Camalet, J.C. Lacroix, S. Aeiyach, K. Chane-Ching and P.C. Lacaze, *Synth. Met.*, **93**, 133 (1998); https://doi.org/10.1016/S0379-6779(97)04099-X
22. A.T. Özyılmaz, T. Tüken, B. Yazıcı and M. Erbil, *Prog. Org. Coat.*, **52**, 92 (2005); https://doi.org/10.1016/j.porgcoat.2004.09.003
23. A.T. Ozyilmaz, A. Akdag, I.H. Karahan and G. Ozyilmaz, *Prog. Org. Coat.*, **77**, 872 (2014); https://doi.org/10.1016/j.porgcoat.2014.01.020
24. N.B. Devkota, S. Singh, S. Neupane, D.K. Gupta and A.P. Yadav, *J. Nep. Chem. Soc.*, **35**, 94 (2016).
25. P. Pawar, A.B. Gaikawad and P.P. Patil, *Sci. Technol. Adv. Mater.*, **7**, 732 (2006); https://doi.org/10.1016/j.stam.2006.09.014
26. M. Shabani-Nooshabadi and F. Karimian-Taheri, *RSC Adv.*, **5**, 96601 (2015); https://doi.org/10.1039/C5RA14333K
27. D.K. Gupta, S. Neupane, S. Singh, N. Karki and A.P. Yadav, *Prog. Org. Coat.*, **152**, 106127 (2021); https://doi.org/10.1016/j.porgcoat.2020.106127
28. D.K. Gupta, S. Neupane, S. Singh, N. Karki and A.P. Yadav, *Data Brief*, **35**, 106875 (2021); https://doi.org/10.1016/j.dib.2021.106875
29. D.K. Gupta, S. Neupane, S. Singh and A.P. Yadav, *Indian J. Chem. Technol.*, **29**, 82 (2022); https://doi.org/10.56042/ijct.v29i1.54305
30. S. Neupane, M.Sc. Dissertation, Development of a Windows-Based Program to Control the Analogue Potentiostat in Combination with an ADA Converter, Tri-Chandra Multiple Campus, Tribhuvan University, Nepal (2013).
31. J.L. Camalet, J.C. Lacroix, S. Aeiyach, K. Chane-Ching and P.C. Lacaze, *J. Electroanal. Chem.*, **416**, 179 (1996); https://doi.org/10.1016/S0022-0728(96)01012-1
32. H.J.N.P. Mello and M. Mulato, *Thin Solid Films*, **656**, 14 (2018); https://doi.org/10.1016/j.tsf.2018.04.022
33. J.C. Lacroix, J.L. Camalet, S. Aeiyach, K.I. Chane-Ching, J. Petitjean, E. Chauveau and P.C. Lacaze, *J. Electroanal. Chem.*, **481**, 76 (2000); https://doi.org/10.1016/S0022-0728(99)00490-8
34. A. Eftekhari, *Synth. Met.*, **125**, 295 (2002); https://doi.org/10.1016/S0379-6779(01)00393-9
35. O. Kazum and M.B. Kannan, *Surf. Eng.*, **32**, 607 (2016); https://doi.org/10.1080/02670844.2015.1108071
36. M. Shabani-Nooshabadi, E. Allahyary and Y. Jafari, *Prot. Met. Phys. Chem. Surf.*, **54**, 104 (2018); https://doi.org/10.1134/S2070205118010276
37. S.K. Dhawan and D.C. Trivedi, *Polym. Int.*, **25**, 55 (1991); https://doi.org/10.1002/pi.4990250110
38. A.F. Diaz and J.A. Logan, *J. Electroanal. Chem. Interface Electrochem.*, **111**, 111 (1980); https://doi.org/10.1016/S0022-0728(80)80081-7
39. E.M. Genies and C. Tsintavis, *J. Electroanal. Chem. Interfacial Electrochem.*, **195**, 109 (1985); https://doi.org/10.1016/0022-0728(85)80009-7
40. N. Mahato and M.H. Cho, *Constr. Build. Mater.*, **115**, 618 (2016); https://doi.org/10.1016/j.conbuildmat.2016.04.073
41. M.M. Popović, B.N. Grgur and V.B. Mišković-Stanković, *Prog. Org. Coat.*, **52**, 359 (2005); https://doi.org/10.1016/j.porgcoat.2004.05.009
42. Y. Chen, X.H. Wang, J. Li, J.L. Lu and F.S. Wang, *Corros. Sci.*, **49**, 3052 (2007); https://doi.org/10.1016/j.corsci.2006.11.007
43. A. Yağan, N.Ö. Pekmez and A. Yıldız, *Prog. Org. Coat.*, **59**, 297 (2007); https://doi.org/10.1016/j.porgcoat.2007.04.006